

A Three-Dimensional Potential-Based analysis for Partial cavitating Flow around Projectiles with Various Head Using BEM

Mahdi Norouzi¹, Mahmoud Pasandideh-fard²

¹Assist. Prof., Department of Mechanical Engineering, Larestan University, Lar, Iran

²Prof., Department of Mechanical Engineering, Ferdowsi University of Mashhad, Mashhad, Iran

*Corresponding author: norouzi347@yahoo.com

Received: 08/05/2023 Revised: 09/16/2023 Accepted: 12/26/2023

Abstract

In this paper, a three-dimensional code has been developed to simulate the partial cavitating flow around projectiles with various heads (blunt, hemispherical, and conical) using the Boundary Element Method, BEM. For this purpose, after generating the geometry using quadrilateral elements, using the integral expression of Green's theory, source and dipole have been distributed on elements, and employing an iterative algorithm, the simulation is performed and the predictions are compared with the available experimental data and other numerical results. Despite the low computational cost of this method, the results have a high accuracy and convergence rate. One of the main contributions of this work is to present a correlation between the properties of cavity around projectiles with different heads ($0.075 \leq \sigma \leq 0.5$). Analysis of the results shows that the method has a suitable ability to predict the properties of cavitation flow at non-zero angles of attack (up to 8°) in the shortest time. Of course, by increasing the angle of attack and getting away from the potential assumption, the results are associated with some errors (15% in geometrical characteristics and 12% in aerodynamic coefficient). Due to high convergence rate and acceptable accuracy, this method can be used for initial stage of design and also optimization of under-water projectiles with cavitation.

Keywords: Partial Cavitation, Boundary Element Method, Angel of Attack, Blunt-Head, Hemispherical-Head, Conical-Head

1. Introduction

The occurrence of cavitation around sub-surface projectiles can lead to a fundamental reduction of the drag, and as a result, an increase in its velocity and efficiency. The most important dimensionless quantity in the analysis of cavitation flows is the "cavitation number" which, along with the geometry and other characteristics of the flow, expresses the regime and type of the cavitation. One of the effective methods for cavitation analysis over various bodies is the Boundary Element Method (BEM). This method is based on the dividing boundaries of geometry into the elements, the distribution of potential flow components (such as source, dipole and vortex) on each of the elements, using integral equations (such as Green). Then by applying this integral equation with suitable boundary conditions on each of the elements, building and solving the system of equations, the power of potential elements and then their velocity and pressure are found [1, 2].

For the first time, Uhlman [3] used a velocity-based nonlinear BEM to solve the 2D partial cavitating flows around hydrofoil. Kinnas and Fine [4] offered another nonlinear BEM based on potential to solve partial

cavitating flow on 2D hydrofoils. The convergence and accuracy of potential-based BEM [4] were better than those of the velocity-based BEM [3].

Researches of Fine and Kinnas became the basis for the development of 3D BEM in partial cavitation analysis. During the last ten years, research in the field of cavitation using the BEM has often been directed towards increasing the speed of analysis and geometry optimization. In 2012, Rashidi and Pasandideh-Fard [5] presented the optimal head-shape of axisymmetric projectiles based on the lowest drag coefficient using BEM. Norouzi et al. [6] presented a quasi-3D BEM algorithm to simulate partial cavitation around projectiles with an elliptical cross-section. In 2022, Moltani et al. [7] investigated the wave characteristics and wave resistance of an underwater vehicle with control surface near the free surface using a 3D BEM algorithm.

A review of studies that have used the BEM for cavitation analysis shows that the most researches in this field, have focused on the simulation on cavitating flows around hydrofoils and propellers, and less has been devoted to the analysis of the cavitation flow around projectiles; a few available BEM studies related to the projectiles have been 2D or axisymmetric model.

On the other hand, the functional conditions of real projectiles such as elliptical cavitator or non-zero angles of attack make the 3D analysis of projectiles inevitable. In present work, a 3D BEM algorithm has been performed to simulate the cavitating flows around blunt, conical (with a cone angle of 45°) and hemispherical-head and the results have been validated with experimental data and other numerical analyzes.

2. Governing equations and solution conditions

In this research, according to the investigated geometries (cylinders with the blunt, hemispherical and conical-head), quadrilateral elements with four control points have been used. The derivation of the 3D equations of present BEM starts with the basic assumption that the flow over the body/cavity surfaces is inviscid, incompressible, steady and irrotational. The basic condition of using this method is that the flow to be potential. Experimental studies of Labertaux et al. [8] confirms that the flow around cavity in most of regions is reasonably approximately a potential one.

The present BEM is based on Green Theorem. This theorem states that every incompressible and irrotational flow can be simulated by source, dipole, or vortex distribution on its boundary surfaces.

In Green's theory, the triple integral over the volume becomes a double integral over the boundaries. Therefore, in Green's integral, only the potential components that create the boundaries appear as "disturbance potential" and the free flow potential is applied to the surfaces as boundary conditions. Thus, the total (ϕ) and disturbance (ϕ_p) potentials are related by:

$$\phi = \vec{U}_\infty \cdot \vec{R} + \phi_p \quad (1)$$

Where the first term on the right, $\vec{U}_\infty \cdot \vec{R}$, is the free stream potential. \vec{U}_∞ can be introduced as a uniform or non-uniform flows. The integral expression of the Green's theory is a potential-based equation that uses the distribution of the 3D source and dipole on the boundaries of the solution domain for simulation:

$$\phi(x) = \int_S \left[\phi(\tilde{x}) \frac{\partial G(x, \tilde{x})}{\partial n_{\tilde{x}}} - G(x, \tilde{x}) \frac{\partial \phi(\tilde{x})}{\partial n_{\tilde{x}}} \right] dS \quad (2)$$

Where $G(x, \tilde{x})$ is the potential of a source and $\partial G(x, \tilde{x})/\partial n_{\tilde{x}}$ is its normal derivative, that is, the potential of a dipole. These two 3D potentials are defined as follows:

$$G(x, \tilde{x}) = \frac{1}{4\pi r(x, \tilde{x})}, \quad r(x, \tilde{x}) = |r| = |x - \tilde{x}| \quad (3)$$

$$\frac{\partial G(x, \tilde{x})}{\partial n_x} = -\frac{1}{4\pi |x - \tilde{x}|^3} r(x, \tilde{x}) \cdot n_x \quad (4)$$

Where x is the position vector of a point in domain that feels the effect of potential components distributed on the elements (field point) and \tilde{x} is the position vector of a point on the elements, on which the potential components are located and affects the points of the field (source point). Also n_x is the normal vector to the outward surfaces at \tilde{x} . $\phi(\tilde{x})$ is the dipole strength and $\partial \phi(x)/\partial n_{\tilde{x}}$ is the 3D spring strength.

Kinematic Boundary Condition on the Body/Cavity Surface: The surface impenetrability condition requires flow to have no normal component on the body surface. It means that flow on the body/cavity surface has only the tangent component:

$$\frac{\partial \phi}{\partial n} = -\frac{\partial(U_\infty \cdot R)}{\partial n} \quad \text{on } S_B \cup S_C \quad (5)$$

Where n is the unit vector normal to the body/cavity surface.

Cavity thickness: Using the cavity surface impenetrability condition, the cavity thickness is defined as follows:

$$\frac{\partial \eta}{\partial s_1} [V_{s_1} - V_{s_2} \cos \theta] + \frac{\partial \eta}{\partial s_2} [V_{s_2} - V_{s_1} \cos \theta] = V_{s_3} \sin^2 \theta \quad (6)$$

Where η is the cavity thickness that is defined based on two tangential components of the surface, s_1 and s_2 , and a normal component to the surface, s_3 . Actually, Equation 3 is the kinematic boundary condition on the cavity.

Dynamic Boundary Condition on the Cavity Surface: Using Bernoulli's equation, dynamic boundary condition on the cavity surface is proved as follows:

$$\frac{\partial \phi}{\partial s_1} = V_{s_2} \cos \theta + \sin \theta \sqrt{U_\infty^2 (1 + \sigma) - V_{s_2}^2} - \vec{U}_\infty \cdot t_1 \quad (7)$$

Using (7), the potential (ϕ) of cavity surface elements will be determined. Equation (7) is used to the Green's integral equation as a known boundary condition on the cavity surface.

According to the experimental observations of Arakri [9], considering minimum C_p as the attachment point of the cavity is a choice close to reality. In this research, the minimum C_p is first obtained by using C_p due to solve without cavitation flow. A simple closing model is also used to close the end of the cavity.

The solution algorithm is such that in the first iteration, an initial length is assumed for the cavity created on each strip and based on this, the system of equations is solved, and the thickness of the cavity at the center point of each cavity element is calculated. Along each strip, when the cavity thickness on the last element of the cavity is equal to zero, it can be said that the solution has converged for the strip. If this condition is

satisfied for all strips of the geometry, the solution is converged; otherwise, using the Newton-Raphson method, the length of the cavity is modified and the equations are solved until the mentioned condition is satisfied in all strips.

3. Results and discussion

3.1. Flow without cavitation: In Figure 1, the distribution diagram of pressure coefficient versus the length traveled on a hemispherical-head cylinder with a diameter of 1 and a length of 10, at $\alpha = 0^\circ$, is compared with the Experimental results [10]. The agreement of the present BEM results with the experimental results is clearly evident.

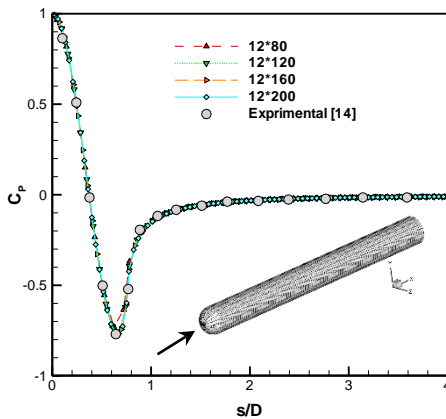


Figure 1. Distribution of pressure coefficient (C_p) versus the length traveled on a hemispherical-head cylinder (without cavitation) in comparison to experimental data [10].

3.2. Partial cavitation over various cylinders: In the current research, a cylindrical geometry with a diameter 1 and a minimum length of 10 is connected to three blunt, hemispherical and conical-head (with a cone angle of 45°). As an example, in Figure 2, the result of partial cavity around a blunt-head cylinder of the present analysis (lower half of the figure) is compared to the results of mixture method [11] (upper half of the figure) modeled by the Fluent software for cavitation number of 0.2. In the analysis by the mixture method, the RSM turbulence model has been used. According to Figure 2, the geometry of the cavity in the two methods are in good agreement with each other.

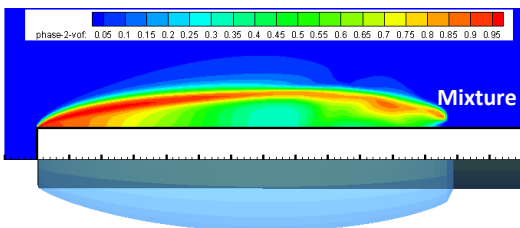


Figure 2. Comparison the partial cavitation of present BEM (lower half) and Mixture model (upper half) [11] around a blunt-head cylinder at $\sigma = 0.2$.

In Figure 3, the distribution of the pressure coefficient (C_p) on the cylindrical bodies with blunt, conical (with a cone angle of 45°) and hemispherical-head resulting from the present analysis is compared with the experimental results [12] in the various cavitation numbers. According to the figure 4, the present results follow the experimental data with a very good match to the end region of the cavity; but at the end of the cavity region, the slope and the maximum pressure coefficient do not match with the experimental data [12]. This is due to the stagnation point that appears in the process of implementing the simple closure model. Of course, due to the limited area of this overshoot, its effects on the aerodynamic coefficients is limited.

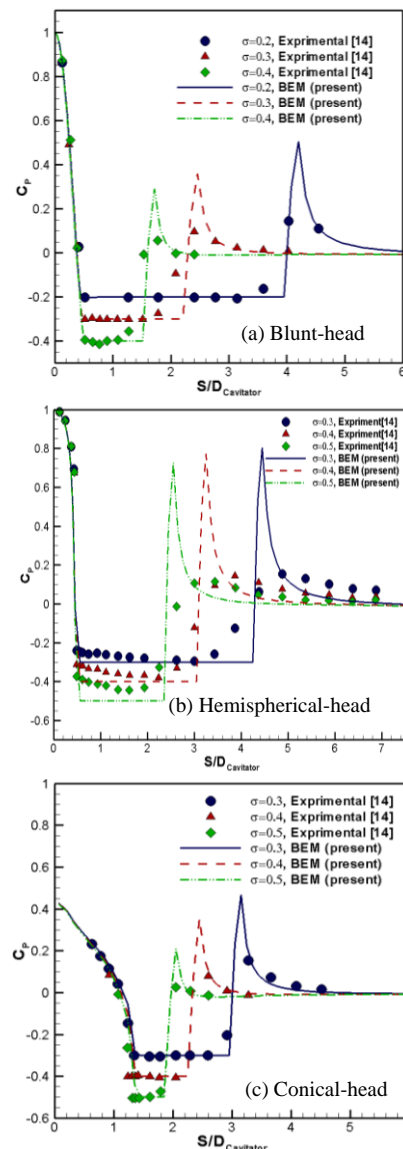


Figure 3. Distribution of pressure coefficient (C_p) versus the length traveled on a strip of the various cylinders with (a) blunt, (b) hemispherical, and (c) conical-head cylinders in comparison to experimental data [10].

The investigation of the partial cavity created around the three investigated geometries in different cavitation numbers confirms the existence of a power relationship

between the cavity length and the maximum thickness of the cavity with the cavitation number as $A\sigma^{-B}$, where σ is the cavitation number. Based on this, by fitting a curve from the results of the present BEM, the relationship between the dimensionless length of the cavity and the maximum thickness of the cavity in terms of the cavitation number for the cylinder with blunt, conical and hemispherical-head is presented in Table 1. It is one of the innovations of this research, which are valid for cavitation numbers in the range of 0.075 to 0.5.

Table 1. The presented power relations between the length and the maximum thickness of the cavity versus σ for various head shapes in forms of $A\sigma^{-B}$ and in the range of $0.075 \leq \sigma \leq 0.5$

	HEAD	A	B
$\frac{L_{cav.}}{D_{cavitator}}$	Blunt	0.785	1.31
	Hemispherical	0.295	1.51
	Conical	0.284	1.47
$\frac{H_{cav.,Max}}{D_{cavitator}}$	Blunt	0.115	1.09
	Hemispherical	0.015	1.60
	Conical	0.027	1.26

In Figure 4, the results of the present analysis for the cavitation flow around a cylinder with a length of 15 at angles of attack of 4 and 8 degrees at a cavitation number of 0.17 are compared with the results of Fluent results using the mixture model. According to the figure, the length and thickness of the cavity resulting from the BEM is about 15% larger than the cavity length resulting from the mixture numerical method, which is due to the potential nature of the BEM. The axial aerodynamic coefficient in the two analyses, except for the angle of 8 degrees on the projectile's head, has an acceptable compliance, and in the observed exception, the difference between the results of the two analyzes is about 12%.

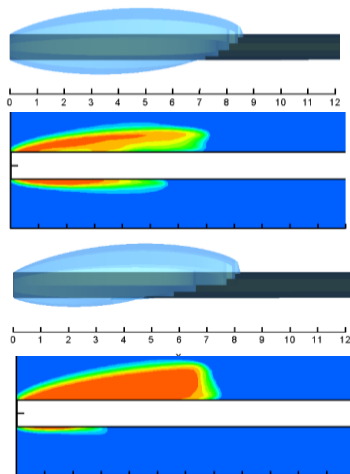


Figure 4. Comparison of the shape of the cavity resulting

from BEM and mixture method (Fluent) around a blunt-head cylinder at the angles of attack of 4 (two upper) and 8 degrees (two downer) at the cavitation number of 0.17.

4. Conclusion

In this research, by using the 3D BEM, the partial cavitation flow around the projectile with different heads and angles of attack was simulated and validated with other numerical and experimental results. Also, at the angle of attack of zero, a series of general power relations were presented for the length and maximum thickness of the cavity in terms of cavitation number. These relations are valid in the range of cavitation numbers from 0.075 to 0.5. Further, the capability of BEM in simulating the partial cavitation flow around the projectiles at non-zero angles of attack was presented. Comparison of the cavity shape and aerodynamic coefficients obtained from BEM and the mixture method (Fluent) at different angles of attack (up to 8° angle of attack) shows that this method has a suitable capability and speed in predicting the flow properties with cavitation. Of course, as the angle of attack increases to higher values, which are used rarely, the results will be accompanied by some error. Very high speed of convergence, suitable flexibility of the solution algorithm and acceptable results are the characteristics of the BEM presented in this research.

5. References

- [1] Barazandeh H, Jafari I (2019) *Experimental Investigation of Cavitation Phenomena around the Body with the Conic Nose and Cylindrical After body*. *Journal of Solid and Fluid Mechanics*, 9(2), pp. 249-259.
- [2] Norouzi M (2016) *3D Simulation of Partial Cavitating Flows over Projectiles at Different Angles of Attack Using Potential Based Boundary Element Method*. PhD thesis, Ferdowsi university of Mashhad.
- [3] Uhlman JS (1987) *The surface singularity method applied to partially cavitating hydrofoils*, *Journal of Ship Research*, Vol. 31, No. 2, pp. 107-124.
- [4] Kinnas SA, Fine NE (1990) *Non-linear analysis of the flow around partially or supercavitating hydrofoils by a potential based panel method*, In *Proceedings of the IABEM-90 Symposium of the International Association for Boundary Element Methods*, Rome, Italy.
- [5] Rashidi I, Passandideh-Fard Mo, Passandideh-Fard Ma (2012) *The Optimum Design of a Cavitator for High-Speed Axisymmetric Bodies in Partially Cavitating Flows*, *Journal of Fluids Engineering*, Vol. 135, No.1:011301.
- [6] M. Nouroozi M, Pasandidehfard M, Djavarehshkian MH (2016) *Simulation of partial and supercavitating flows around axisymmetric and quasi-3D bodies by boundary element method using simple and reentrant jet models at the closure zone of cavity*, *Mathematical Problems in Engineering*, Volume 2016 | Article ID 1593849.
- [7] Moltani Shahrakht AA, Pasandideh-Fard M, Maghrebi MJ (2022) *Investigation of Wave Characteristics and Wave Resistance of an Underwater vehicle with Control Surface Near the Free Surface*, *Journal of Solid and Fluid Mechanics*, 12(2), 65-79.
- [8] Labertaux KR, Ceccio SL (2001) *Partial cavity flows (Part I), Cavities forming on models without span wise variation*, *J. Fluid Mech.*, Vol. 431, pp. 1-41.

- [9] Arakeri VH (1975) *Viscous Effects on the Position of Cavitation Separation from Smooth Bodies*, Journal of Fluid Mechanics, Vol. 68, No. 4, pp.779–799.
- [10] Currie IG (2001) *Fundamental Mechanics of Fluids*, Third Edition, University of Toronto, Canada.
- [11] De Lange DF, De Bruin GJ (1998) *Sheet Cavitation Cloud Cavitation and Re-entrant Jet and Three-Dimensionality*, Netherlands, pp. 92-95.
- [12] Rouse H, Mc Nown JS (1984) *Cavitation and Pressure Distribution, Head Forms at Zero angle of Yaw*, Stud. Engrg., State University of Iowa, Vol. 32.